

Supporting Information

Controlling Screw Dislocation Evolutions towards High Homogeneous Quasi-Two-Dimensional $(\text{BA})_2(\text{MA})_{n-1}\text{Pb}_n\text{I}_{3n+1}$ Single Crystals for High Response Photo-detectors

Qing Yao¹, Jie Zhang¹, Kaiyu Wang¹, Changqian Li¹, Chenyu Shang¹, Haiqing Sun¹, Weiwei Zhang¹, Tianliang Zhou^{2,*}, Huiling Zhu^{1,*}, Jianxu Ding^{1,*}

1. College of Materials Science and Engineering, Shandong University of Science and Technology, Qingdao 266590, China;
2. College of Materials, Xiamen University, Xiamen 361005, China;

Corresponding authors:

Tianliang Zhou- College of Materials, Xiamen University, Xiamen 361005, China;
orcid.org/0000-0002-0086-084X; Email: bible2@163.com

Huiling Zhu- College of Materials Science and Engineering, Shandong University of Science and Technology, Qingdao 266590, China; orcid.org/0000-0002-5698-1026;
Email: skdzhl@sdu.edu.cn

Jianxu Ding- College of Materials Science and Engineering, Shandong University of Science and Technology, Qingdao 266590, China; orcid.org/0000-0001-5662-2683;
Email: dingjianxu@sdu.edu.cn

1. Descriptions of the raw materials purity

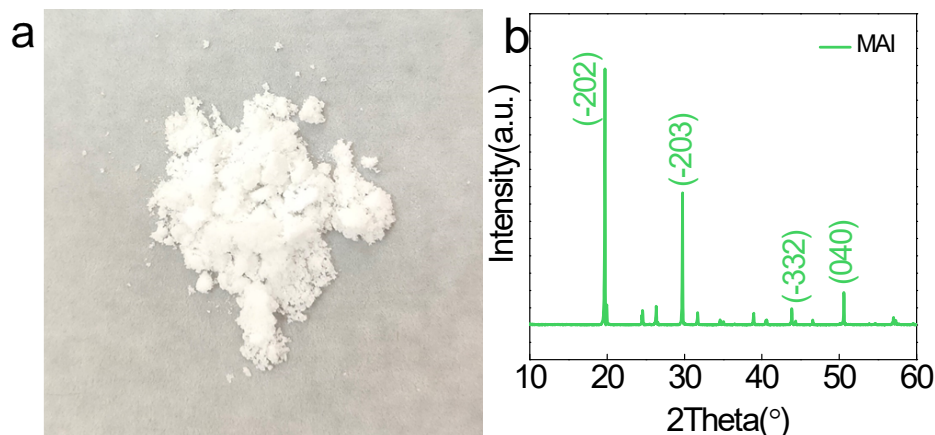


Figure S1 (a-b) Photograph and XRD pattern of MAI powders.

The synthesis process of MAI powders: Methylamine CH_3NH_2 solution and hydroiodic acid HI are reacted in an ice-water bath at a volume ratio of 6:5. After reacting for 4 hours, the mixed solution was sealed at 60°C for 24 hours. The crystallization of MAI is achieved by evaporating water at 60°C to obtain white MAI powder (Figure S1a). Figure S1b shows the XRD pattern of MAI powder.

2. Photographs of BMPI solution preparation

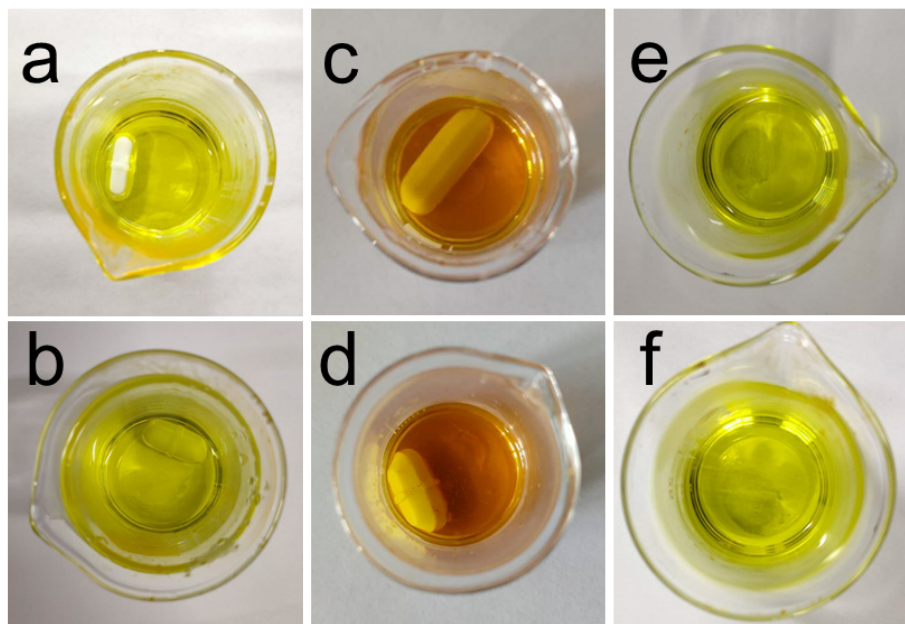


Figure S2 (a-b) Photographs of I solution; (c-d) Photographs of II solution; (e-f) Photographs of crystal growth solution.

3. Photographs of BMPI perovskite SCs growth

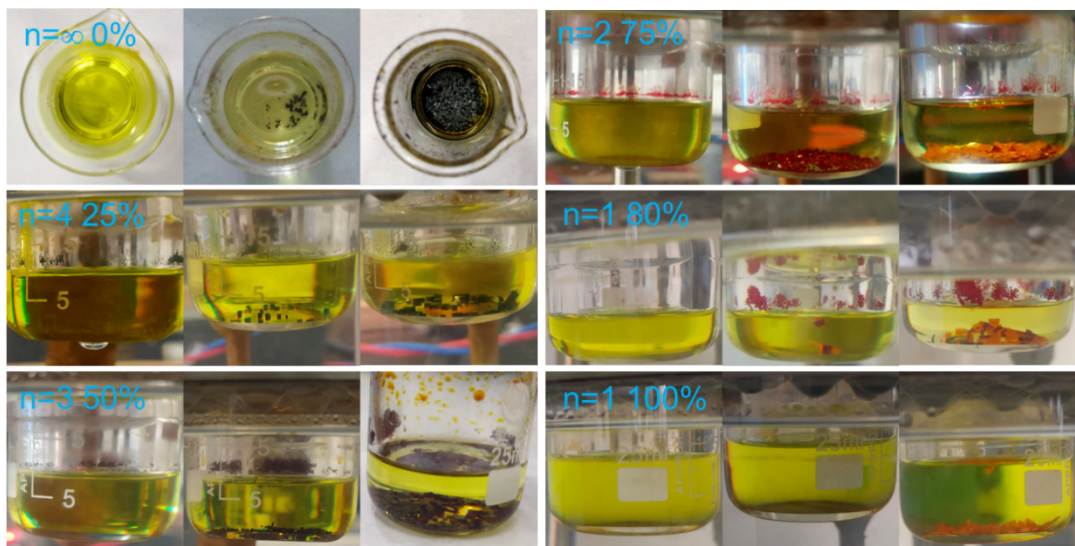


Figure S3 Photographs of BMPI ($n=1-4$ and ∞) SCs growth.

4. Crystal data for BMPI ($n=1-4$ and ∞) SCs at 293K

Table S1. Crystal data for BMPI ($n=1-4$ and ∞) SCs at 293K

n values	$n=1$	$n=2$	$n=3$	$n=4$	$n=\infty$
Crystal system	orthorhombic	orthorhombic	orthorhombic	orthorhombic	tetragonal
Space group	Pbca	Cc2m	C2cb	Cc2m	I4/mcm
Color	orange	red	dark red	black	black
a(Å)	8.8555(8)	8.9470(4)	8.9275(6)	8.9274(4)	8.8392(3)
b(Å)	8.6810(8)	39.347(2)	51.959(4)	64.383(3)	8.8392(3)
c(Å)	27.602(3)	8.8589(6)	8.8777(6)	8.8816(4)	12.6948(5)
$\alpha=\beta=\gamma(\text{deg})$	90	90	90	90	90
Volume(Å ³)	2121.89(4)	3118.67(3)	4118.04(5)	5104.9(4)	991.86(6)
Z	8	4	4	4	4
References	[1]	[2]	[2]	[2]	[3]

5. 2D AFM image of heterojunction structures on the (020) surface of BA₂MA₃Pb₄I₁₃ SCs

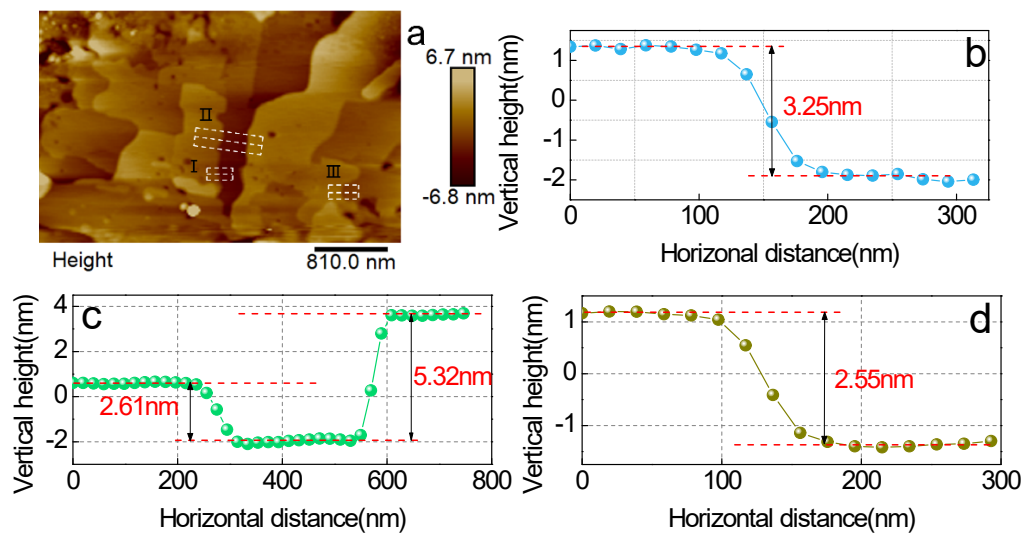


Figure S4. (a) 2D AFM images of heterojunction structures of BA₂MA₃Pb₄I₁₃ SCs; (b-d) step heights.

6. 2D AFM image of BA_2PbI_4 SCs

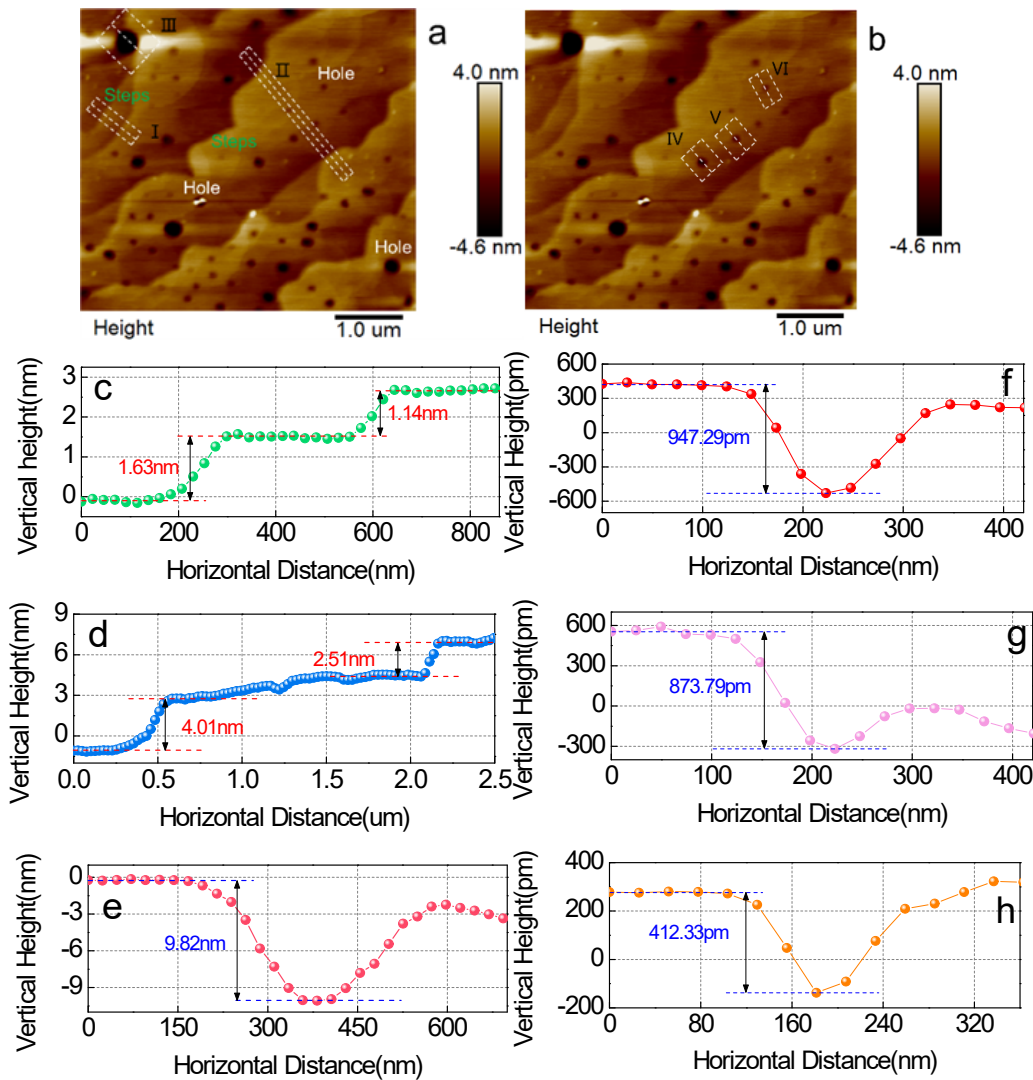


Figure S5. (a-b) 2D AFM image of growth steps and holes on (002) surface of BA_2PbI_4

($\text{BA}=20\%$) SCs; (c-h) step heights and hole depth files of the measured steps and holes.

7. Spiral dislocation diagram of BMPI ($n=2-3$) SCs

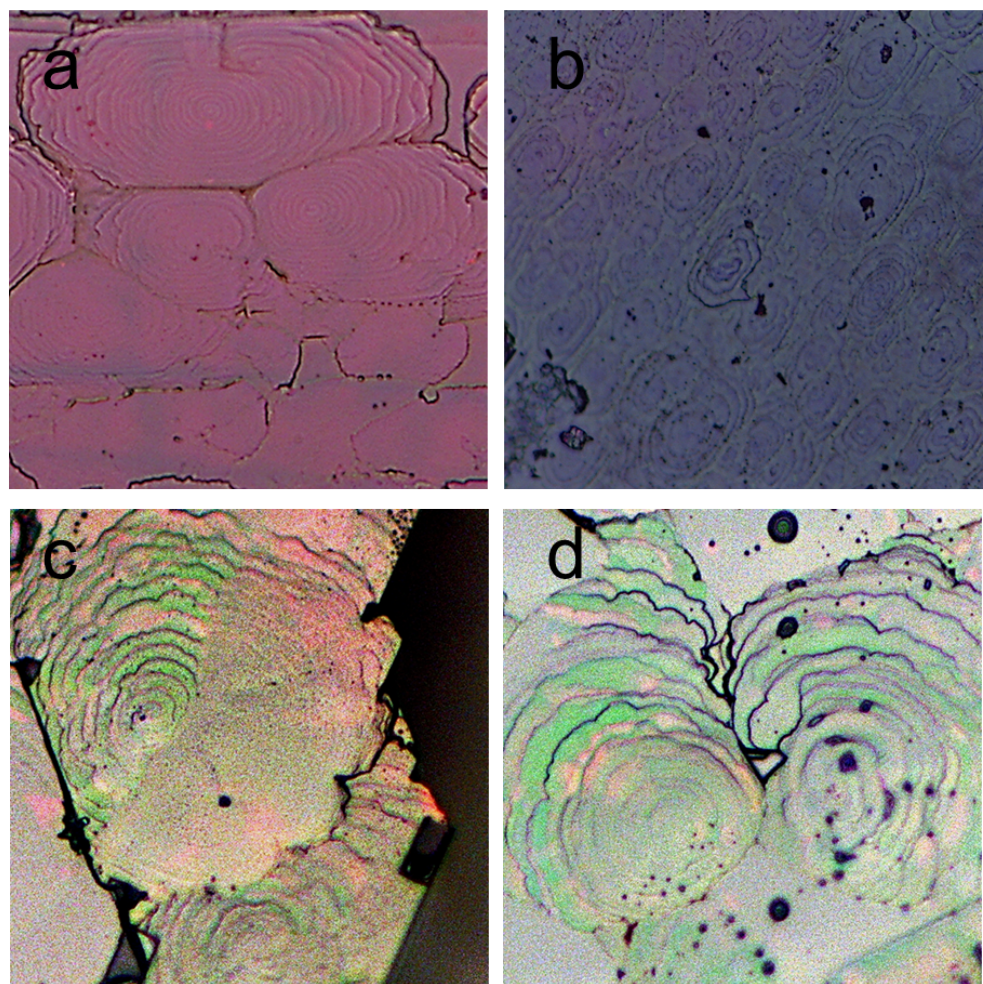


Figure S6. (a-d) Spiral dislocation diagram of BMPI ($n=2-3$) SCs (magnification: 50).

8. 2D AFM layered structure

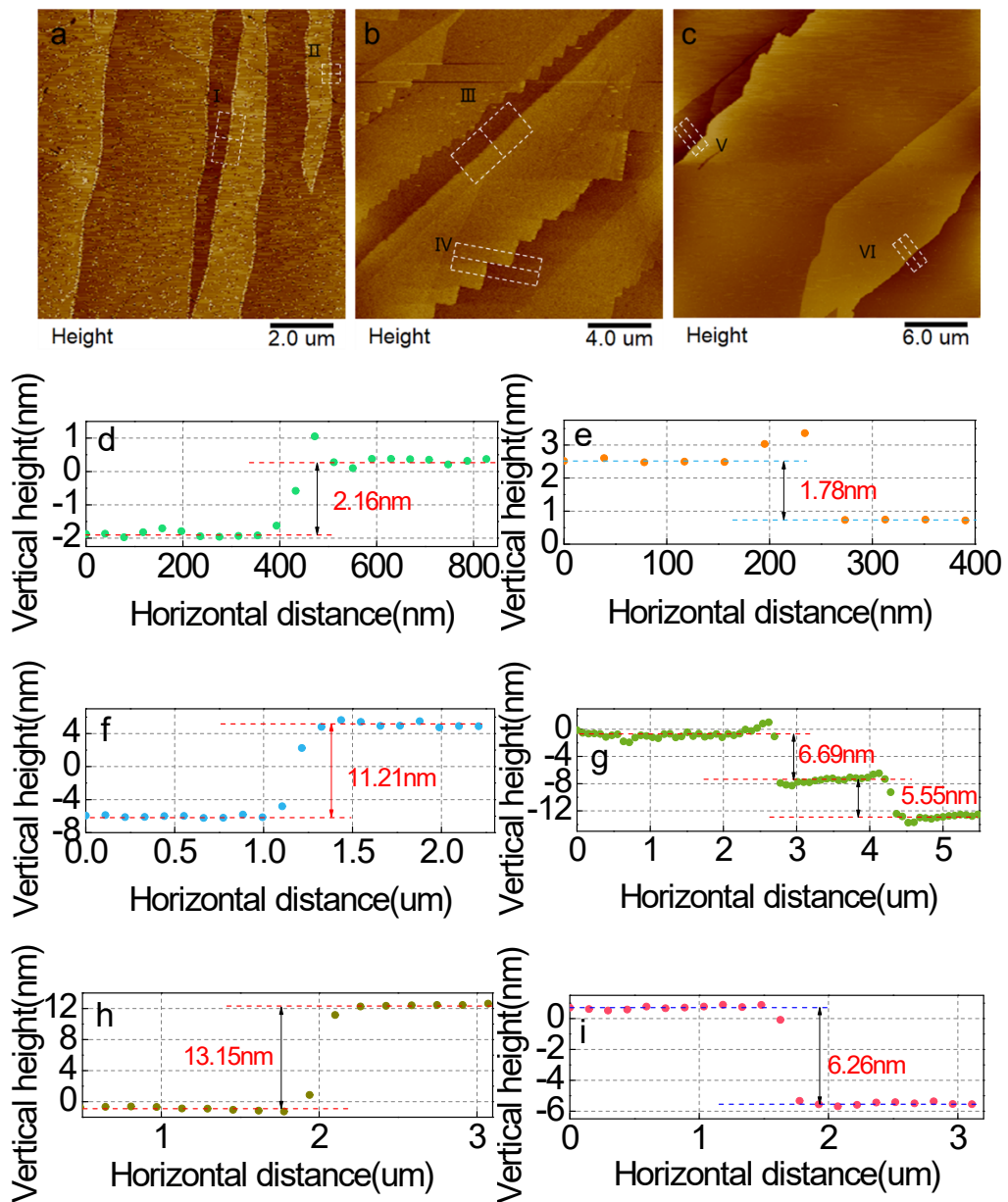


Figure S7. (a-c) 2D AFM layered structure on BMPI ($n=2-4$) SCs (020) surface; (d-i)

The heights between layers of the layered structure on the (020) surface.

9. Length and width of screw dislocation steps

Table S2. Length and width of screw dislocation steps

number	Width (μm)	Length (μm)
1	2.05	2.25
2	2.16	1.72
3	2.37	1.79
4	2.05	2.25
5	1.73	1.72
6	1.51	1.62
7	1.51	1.40
8	1.83	1.62
9	1.62	1.96
10	1.51	1.62
11	1.51	1.29
12	1.62	1.83
13	1.62	1.72
14	1.62	1.79
Average	1.765	1.797

References

- (1) A. M. Sanni, S. Lavan, A. Avramenko, F. A. Rabuffetti, L. Suescun, A. Rury, Room-Temperature Broadband Light Emission from Hybrid Lead Iodide Perovskite-Like Quantum Wells: Terahertz Spectroscopic Investigation of Metastable Defects, *J. Phys. Chem. Lett.*, **2019**, *10*, 1653-1662.
- (2) C. C. Stoumpos, D. H. Cao, D. J. Clark, J. Young, J. M. Rondinelli, J. I. Jang, J. T. Hupp, M. G. Kanatzidis, Ruddlesden-Popper Hybrid Lead Iodide Perovskite 2D Homologous Semiconductors, *Chem. Mater.*, **2016**, *28*, 2852-2867.
- (3) P. S. Whitfield, N. Herron, W. E. Guise, K. Page, Y. Q. Cheng, I. Milas, M. K. Crawford, Structures, Phase Transitions and Tricritical Behavior of the Hybrid Perovskite Methyl Ammonium Lead Iodide, *Sci. Rep.*, **2016**, *6*, 35685.